Cyclone Climatology of the Bering Sea and Its Relation to Sea Ice Extent

JAMES E. OVERLAND AND CAROL H. PEASE

Pacific Marine Environmental Laboratory/NOAA, Seattle, WA 98105

(Manuscript received 27 April 1981, in final form 4 December 1981)

ABSTRACT

A monthly storm-track climatology is derived from monthly maps of cyclone tracks for the winter season, October through March, averaged over 23 years, 1957/58–1979/80, for a 2° latitude × 4° longitude grid bounded by 51°N, 65°N, 157°W and 171°E. There is a decrease in the number of cyclones with latitude in all months and division into two storm tracks, one propagating north-northeast along the Siberian peninsula and one entering the southern Bering Sea on a northeasterly course and either curving northward into the central Bering Sea or continuing parallel to the Aleutian Island chain.

Monthly average ice extents are established for February and March 1958–80 along a line from Norton Sound southwest toward the ice edge, perpendicular to the average maximum extent. Comparison of composite cyclone charts summed over the winter season and over the five heaviest and five lightest ice years shows a shift in cyclone centers toward the west in light ice years. The correlation between maximum seasonal ice extent and the difference between the number of cyclone centers in the eastern minus the western part of the basin over each winter season is 0.71. The relation of sea ice extent and the location of cyclone tracks is consistent with previous observations that advance of the ice edge in the Bering Sea is dominated by wind-driven advection and that southerly winds associated with cyclone tracks to the west inhibit this advance. These results indicate that the interannual variability in seasonal sea-ice extent in the Bering Sea is controlled by an externally determined variation in storm-track position related to large-scale differences in the general circulation. A skewed distribution of ice extents toward heavy ice years, however, suggests the possibility of an oceanographic constraint on the magnitude of extreme seasonal ice extents, such as the inability of melting ice to cool the mixed layer beyond the continental shelf to the freezing point or the increased influence of the northwestward flowing, continental slope current.

1. Introduction

Studies beginning early this century (Brennecke, 1904) have indicated relationships between sea-ice extent and anomalies in sea-level pressure, air temperature and precipitation. It is known that ice growth depends upon such atmospheric parameters as air temperature, wind velocity and cloud cover, and that ice transport depends upon wind and current velocities. On the other hand, sea ice extent and its snow cover modify the surface albedo and reduce the sensible and latent heat flux to the atmosphere from subpolar oceans. The presence of an ice edge produces large horizontal gradients in these fluxes.

Empirical studies of ice extent and atmospheric circulation can be divided into those of regional scale (Wiese, 1924; Schell, 1964; Crane, 1978) and those of hemispheric scale (Schwerdtfeger and Kachelhoffer, 1973; Walsh and Johnson, 1979b). In the Northern Hemisphere, study of the large-scale problem is made complex by having both sea-ice zones and land masses along a given latitude circle. Any interannual variability in sea ice extent will force the atmosphere only in specific locations. The problem of feedback is also complicated by the different kinds of sea ice forcing active in different parts of the hemisphere. Ice in the East Greenland Sea is influenced by ocean currents (Wadhams, 1981). Rogers (1978) has shown that the number of thawing degree days is the parameter most highly correlated with location of the summertime ice margin in the Beaufort Sea. Thus, there exists a need to investigate regional interaction as an aid to understanding hemispheric-scale feedback in addition to more direct application to local ice-edge forecasting.

In this century the Bering Sea has been completely ice-free in summer. In October and November ice forms *in situ* along the coasts in the northern part of the basin. Under the influence of predominantly northeasterly winds, this ice is driven toward the southwest creating polynyas along the southern side of Seward Peninsula and St. Lawrence Island (Fig. 1). These coastal polynyas act as production sites for new ice during most of the winter (Muench and Ahlnäs, 1976; McNutt, 1981). The leading floes along the edge of the pack ice are advected into water that is warmer than the freezing point, and the floes melt. This meltwater combines with the large, sensible heat flux from the ocean caused by the cold off-ice winds to cool the ocean and allow the pack extent

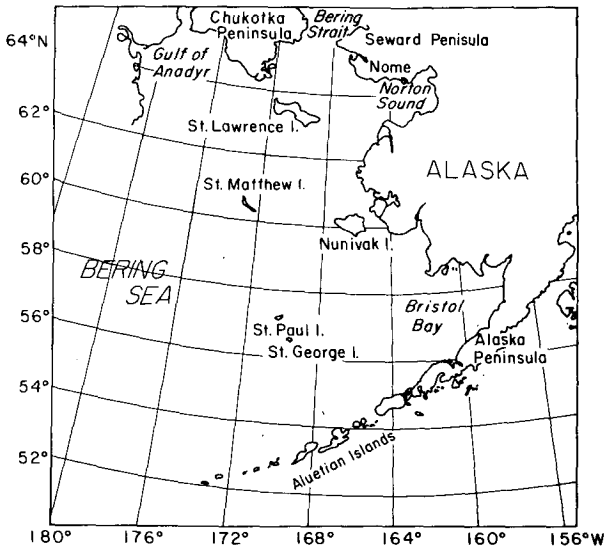

FIG. 1. Location map for eastern Bering Sea.

to advance. Thus, in midwinter, movement characteristics of the ice can be described as a kind of conveyor belt: ice grows primarily in the north, is advected by wind stress generally southward, and decays at the southern thermodynamic limit. The ice may replace itself two to five times during a winter season by this mechanism, which represents a substantial latitudinal heat flux (Pease, 1980). Advection of sea ice by currents is of secondary importance as tidal currents dominate the horizontal kinetic energy on the continental shelf and vector mean flow is 1–5 cm s^{-1} toward the north or northwest (Kinder and Schumacherr, 1981b). In a year of heavy ice, the pack will reach St. Paul Island and beyond, while in a light ice year the pack may reach only beyond St. Matthew and Nunivak Islands (Webster, 1981). Maximum extent occurs between mid-February and late March (Dunbar, 1967). At approximately the time of the vernal equinox the radiation balance at the surface of the ice changes so that the ice melts over most of the basin even under continued northeasterly winds. Increased south-to-southeasterly winds also contribute to spring decay. Sea ice is absent by the end of June.

Although many of the individual features of the dynamics and thermodynamics of Bering Sea ice have been explored and the seasonal cycle prescribed (Niebauer, 1980), the nature of the relation between interannual variations in sea ice extent and atmospheric forcing has not been discussed in detail for a long time series other than as a part of the study by Johnson (1980). Rapid ice advance with northeasterly winds generally occurs during episodes when arctic high pressure dominates the northern Bering Sea. The ice advance is interrupted by penetration of cyclone activity into the Bering Sea bringing warm, moist, oceanic air masses with southerly wind (Pease and Muench, 1981). We take as a working hypothesis that an increase in the frequency of cyclones and of westerly tracks of cyclones will reduce the total duration of northeasterly winds during an ice growth season and will provide an index to determine the overall ice maximum extent in any given year.

2. Cyclone climatology

There are three basic approaches to generalize the synoptic variability in a given region: the use of a synoptic climatology (Barry and Perry, 1973), which regards patterns of weather as an implicit function of the static sea-level pressure distribution; the kinematic approach, in which synoptic weather maps are classified in terms of principal storm tracks; and variance of sea-level pressure, which is generally preferred for hemispheric studies (Blackmon *et al.*, 1977). A synoptic climatology is most appropriate in regions such as the Gulf of Alaska, where a portion of the sea-level pressure features form or decay *in situ* or are persistent (Suckling and Hay, 1978; Overland and Hiester, 1980) and was used for the sea-ice extent study for Davis Strait by Crane (1978). The two synoptic climatologies covering the northern Bering Sea (Putnins, 1966; Barry, 1977) indicate a major first weather type associated with arctic high pressure. The remaining weather types, however, have nearly the same frequency of occurrence and are arbitrary in location, indicating that there is not a strong locational preference for synoptic features. The latter observation and a previous cyclone track study by Klein (1957) suggest that a storm track climatology is a more appropriate technique for summarizing synoptic variability in the central Bering Sea.

Previous analyses of both cyclone and anticyclone frequency patterns have included the Bering Sea only in studies of larger areas—as in the hemispheric studies of Petterssen (1956), Klein (1957), and in the North Pacific/North America study of Blasing and Fritts (1976). Klein used a grid of 5° latitude × 5° longitude to determine the spatial distribution of cyclone and anti-cyclone frequencies for individual months based upon the daily synoptic series for 1899–1939. He constructed principal tracks drawn through axes of maximum frequency. Blasing and Fritts (1976) determined a synoptic climatology based upon sea-level pressure for winter, December–February, and then produced cyclone frequency charts for each of their winter types; their two major weather types based upon 68 years of data show a northwest–southeast shift in a single principal storm track over the Bering Sea.

The data used in this study were derived from monthly maps of cyclone tracks published in the

Mariners Weather Log for November 1957–March 1980. Locations for pressure centers are given on these charts for 0000 and 1200 GMT for centers having at least one closed isobar and whose lifetimes are at least 24 h. Storm tracks for October 1957 were computed directly from daily sea-level pressure charts to complete the ice year for winter 1957/58. To study horizontal distributions, 2° latitude × 4° longitude grids were prepared, and cyclone frequencies were determined by counting the number of cyclone tracks that passed through each quadrangle in a particular month and year. Although the area enclosed by the quadrangles decreases with increasing latitude, no areal corrections are made (Zishka and Smith, 1980; Hayden, 1981). Quadrangles of this size were used to avoid qualitatively noisy fields which resulted from using smaller areas.

Fig. 2 shows the number of storms passing through each quadrangle for the 23-year period from 1957 to 1979 for the months of October–December and from 1958 to 1980 for January–March. October shows two tracks in the Bering Sea, one starting in

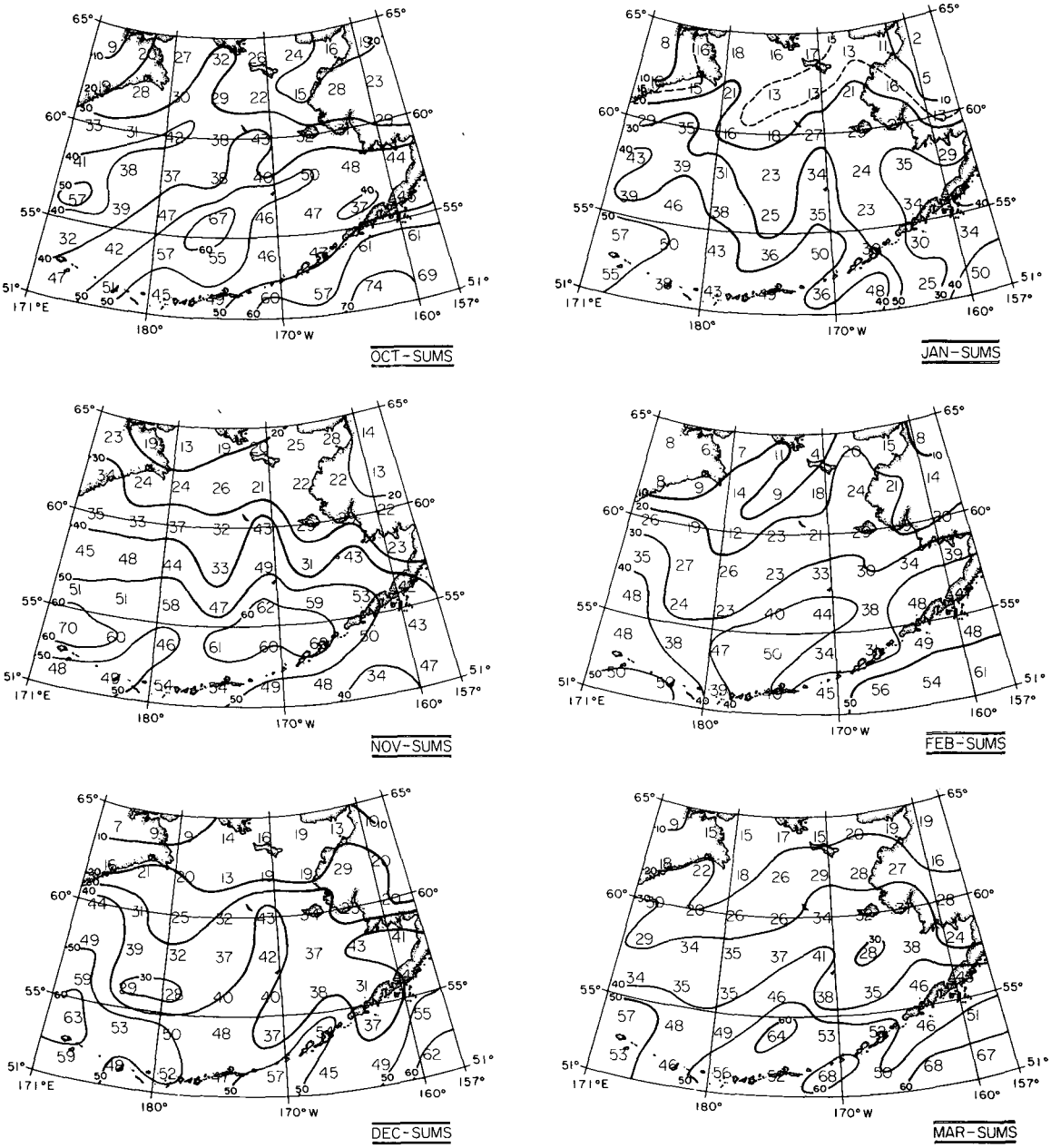

FIG. 2. Storm count by 2° latitude × 4° longitude squares for 23 years—1957–79 (October–December) and 1958–80 (January–March).

the lower left corner at 179°E, 51°N and heading east-northeast parallel to the Aleutian Islands. The second track enters at 171°E, 56°N and curves northward toward Bering Strait and the Chukotka Peninsula. The number of storms reaching north of 60°N decreases in following months because the dominant Siberian high pressure is established in the northwest corner of the region. November has a maximum at 170°W, 55°N with one track entering from the west and then either continuing parallel to the Aleutians or curving north into the Bering between 160 and 180°W. Northerly tracks both along 170°W and 175°E persist through February; however, the absolute frequency drops substantially with latitude in all months. The importance of the northern track peaks in January when the frequency along these tracks is of a similar magnitude to that in the eastern part of the Aleutians. This relative lack of storms in the eastern Aleutians in January corresponds to maximum blocking-ridge activity in the North Pacific as given by White and Clark (1975). They show that 29% of the 31 Januaries from 1959 to 1970 had blocking-ridge activity as compared to 10% for the months of December and February.

Fig. 3 shows the zonal average frequencies between 160 and 180°W as a function of month illustrating the latitudinal dependence. These figures have been normalized by month and by area. There is a winter cycle with an overall minimum in January and February. The latitudinal gradient of storms is roughly constant for all months except January, which has a more uniform north–south gradient.

3. Sea ice data

The ice extent data available for the Bering vary widely in quality and quantity between the early 1950's and the present. Satellite observations of the ice extent are available for 1967 through present. Prior to 1967, ice extent was recorded by direct observation from ships or through occasional ice reconnaissance flights by the Navy and others. Most of the available observations of hemispheric ice extent and concentration from 1952 to 1977 have been collected by Walsh and Johnson (1979a, 1979b) and blocked into 1° latitude equivalent areas by month. When no observations were available during a given month for any given area they include their average monthly ice concentration over all years. Unfortunately, they were particularly forced to use this method west of 180°W in the Bering Sea. To avoid biasing our ice extent estimates by their averaging procedure, we calculated ice extent using the Walsh-Johnson data set for winters 1957/58 to 1970/71 along a section of their grid in the eastern Bering Sea, shown in Fig. 4. This section is located approximately along the climatological ice floe trajectory paths from Norton Sound southwest to the ice edge. For winters 1971/72 to 1979/80, we have computed extents from monthly averages of the U.S. Navy/NOAA Joint Ice Center charts. All years have been compared with available naval air reconnaissance data. Table 1 lists our February and March ice extents along the track in Fig. 4 and indicates the five heaviest and five lightest ice years in the record; a

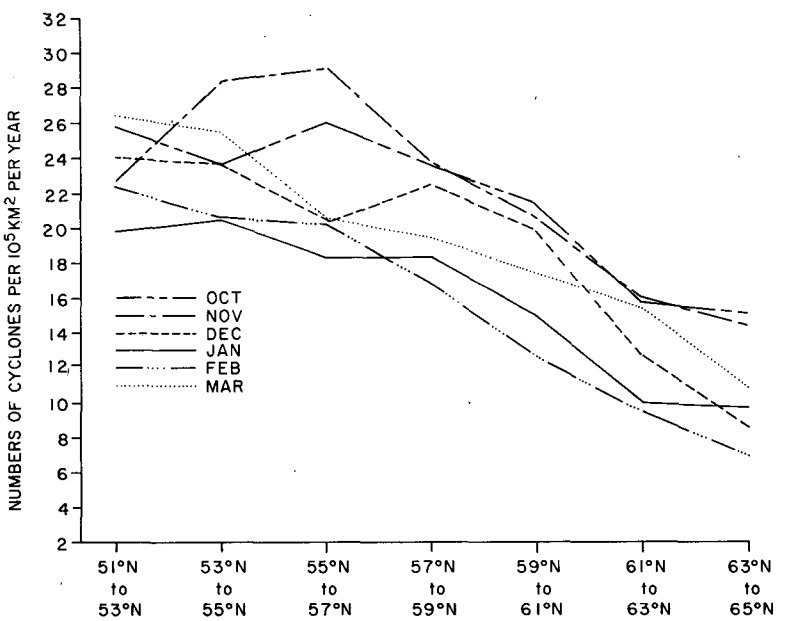

FIG. 3. Storm frequency between 160 and 180°W as a function of month and latitude.

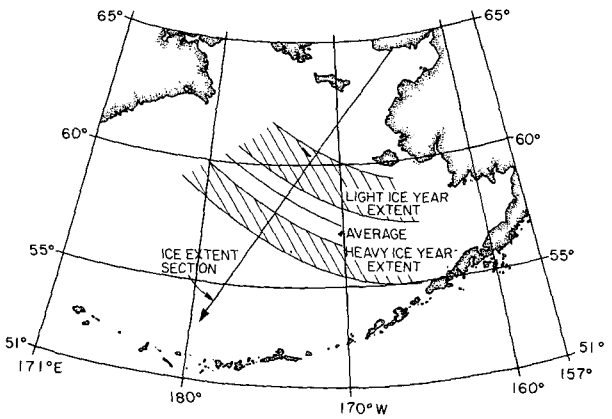

FIG. 4. Section along which maximum ice extents are computed and range of five minimum and maximum ice extents for 1958–80 relative to the section.

TABLE 1. Average February and March ice extent in the Bering Sea along the section shown in Fig. 4.

Year	February extent (km)[5]	March extent (km)[5]	Confidence[4] in extent (km)	Heavy or light ice
1958	930	660	±100	H
1959	550	670	±100	L
1960	700	800	±100	
1961	960	970	±100	H
1962[1]	760	770	±200	
1963	770	810	±100	
1964	1030[2]	930	±100	H
1965	800	800	±100	
1966	465	540	±100	L
1967	660	430	±100	L
1968	860	720	±100	
1969	670	770	±50	
1970	690	800	±50	
1971	870	870	±50	
1972[3]	780	890	±30	
1973	680	870	±30	
1974	800	790	±30	
1975	770	790	±30	
1976	940	910	±30	H
1977	890	830	±30	H
1978	670	750	±30	L
1979	560	650	±30	L
1980	750	780	±30	

[1] No U.S. Navy ice reconnaissance missions were flown in the western Arctic in 1962, so average February and March values are used. Note that this is not the same as the mean maximum extent. See footnote 5.

[2] Revised downward from Walsh and Johnson (1979a) data. The new value is consonant with U.S. Navy ice reconnaissance observations during the winter of 1964.

[3] Values for 1972–80 were obtained by averaging weekly ice extents from analysis maps from the U.S. Navy/NOAA Joint Ice Center in Suitland, MD.

[4] Subjective assessment based on frequency and coverage of the Bering Sea by U.S. Navy ice reconnaissance flights prior to 1969 and thereafter on the resolution and cloud-free coverage by NOAA satellite visual and infrared imagery.

[5] February $\bar{x}$ = 763.4, S.D. = 142.9; March $\bar{x}$ = 774.1, S.D. = 126.5; Maximum, either month: $\bar{x}$ = 812.2, S.D. = 114.5.

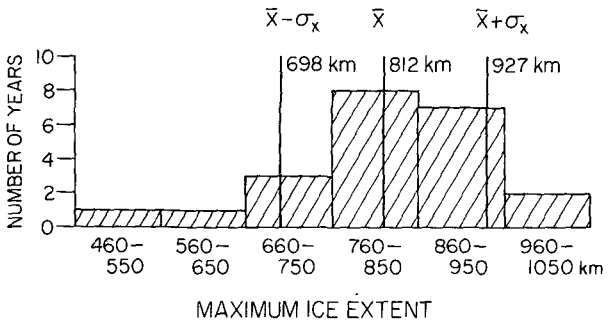

FIG. 5. Distribution of maximum ice extents 1958–80.

plot of their ranges is shown in Fig. 4. Our maximum and minimum years differ from those of Walsh and Johnson (1979b) and Johnson (1980) because of their averaging technique and because they based their maximum extents on January values.

Maximum ice extent occurs most often in February in heavy ice years and in March otherwise. Of the five winters identified in Table 1 as heavy ice years, four have their maximum ice extent in February, while of the five winters identified as light ice years, four have their maximum in March. In fact, only seven of 28 years have maximum extent in February. The variance of the ice extent along our trackline is 28% greater in February than in March. March is the great equalizer: heavy ice in February tends to decline in March, and light ice in February tends to increase in March, although there is an overall bias for maximum in March. The standard deviation of the maximum ice extent is less than the standard deviation in either month.

The distribution of maximum ice extent by 100 km class intervals in Fig. 5 is skewed toward heavy ice years. This may be evidence that there is a constraint on extremely heavy maximum ice extents. Possible constraint mechanisms are: 1) the change in radiation balance at more southerly latitudes as the equinox approaches, 2) increased influence of the northwestward flowing Bering slope current along the shelf break (Kinder and Schumacher, 1981b), and 3) the inability of melting ice to cool the mixed layer to the freezing point beyond the outer continental shelf (Kinder and Schumacher, 1981a).

4. Relation of storm tracks to sea ice extent: qualitative results

To investigate the relationship between storm tracks and sea-ice extent for heavy, light and average ice conditions we summed the number of storms during the five-month ice growth season from October through February (Niebauer, 1980) for each year for each square in our storm track grid. Then we summed over the five heavy years and the five light years as given in Table 1. In addition, we summed

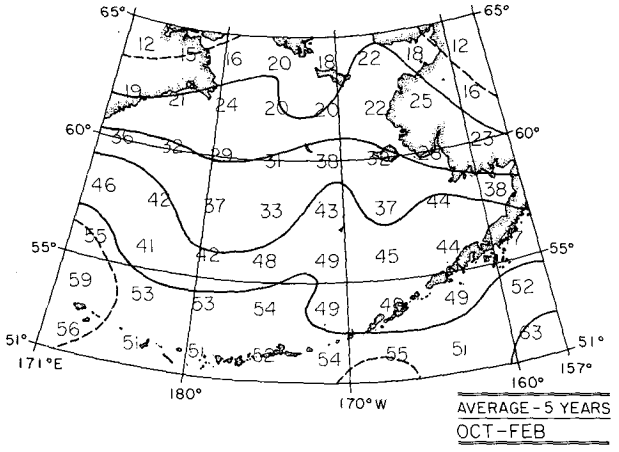

FIG. 6. Average number of storms by 2° latitude × 4° longitude squares for five months (October–February) and five years.

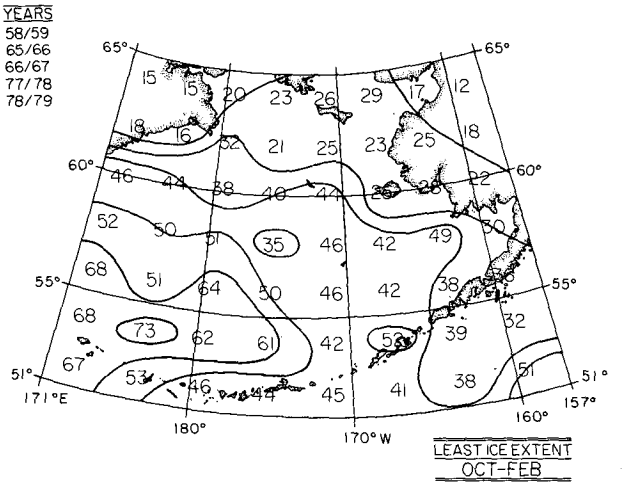

FIG. 8. Storm track counts for the five lightest ice years for months October–February.

all 23 years in the meteorological record, scaled these numbers by dividing the sums by 23, and multiplied by 5 to estimate a mean pattern for the region for comparison to the light and heavy groupings.

In the average five-year storm pattern for October–February given in Fig. 6, storms pass zonally from west to east, with a decrease in storms with increasing latitude, and there is a slight indication that more tracks follow either the Siberian or Alaskan coastline as in the monthly averages. The five heavy ice years (Fig. 7) are characterized by a maximum of storm centers at 170°W, 51°N in the southeast Bering, with fewer storms penetrating north of 60°N than on the average, although secondary tracks along either coast are still present. The light ice years (Fig. 8) are characterized by a maximum of storm centers at 177°E, 54°N in the southwest Bering. The principal track is shifted northward from south of the Aleutians to about 56°N, but there is also an increase in storms in the western portion of the basin at 60°N, and there are more storms throughout the basin than in the average case. The maximum number of storms for both light and heavy ice years occurs in the southern portion of the region beyond the limit of ice extent. The longitude of the maximum number of cyclones and the location of the principal storm track are the major differences between light and heavy ice years. Fig. 9 shows the storm pattern for the years of greatest-minus-least ice extent, which clearly shows the east–west difference in storm track location.

Of the five years identified in Table 1 as heavy ice extent years, 1976/77 was the least significant of the choices. There were other years that were statistically similar, such as 1971/72, and a reanalysis of the cyclone center pattern with 1971/72 instead of

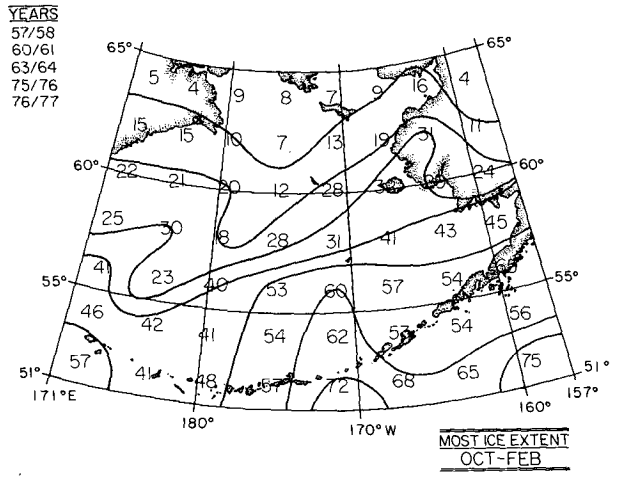

FIG. 7. Storm track counts for the five heaviest ice years for months October through February.

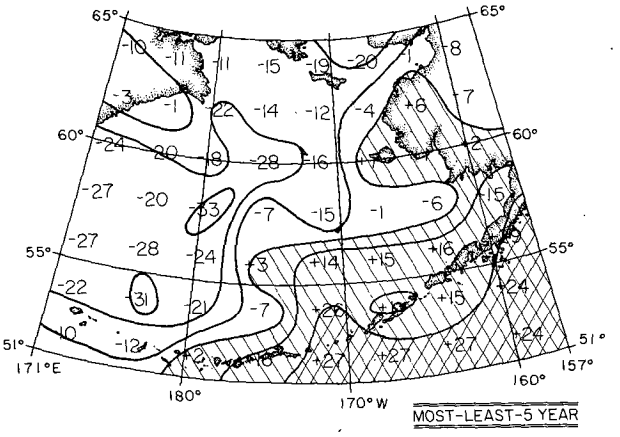

FIG. 9. Maximum ice extent cyclone counts minus minimum ice year counts.

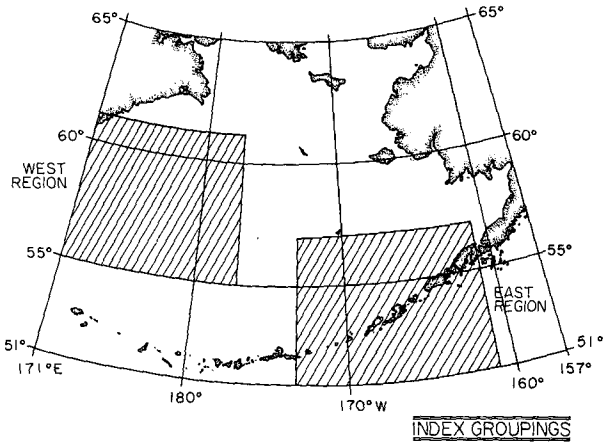

FIG. 10. Regions of cyclone counts for index 1.

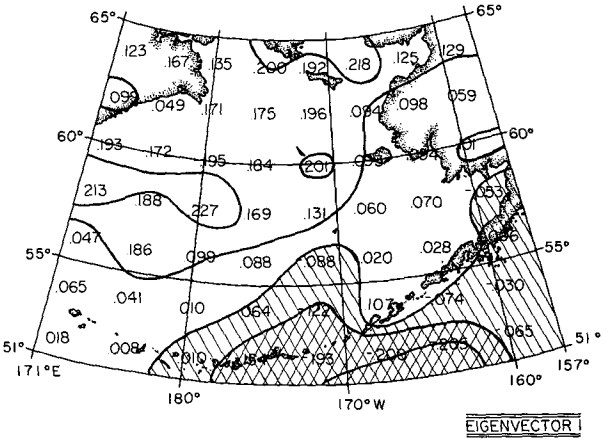

FIG. 11. Largest empirical orthogonal function of cyclone counts October–February for 1957–80.

1976/77 gave results similar to Fig. 7. Likewise, of the five years identified in Table 1 as light ice extent years, 1977/78 was the least significant of the choices. Reanalysis of the storm center pattern with 1968/69 substituted for 1977/78 gave results similar to Fig. 8.

Sea-ice extent in a given winter appears to be primarily controlled by the track of storms entering the Bering Sea and to a lesser extent by the number of storms. This fits surface observations of the dynamical processes controlling sea-ice extent (Pease, 1980). In heavy ice years two situations arise: either storms propagate zonally across the southern Bering and high pressure is established north of the basin, or else storms propagate northward on the Alaskan side of the Bering Sea. Both situations result in advection of cold, dry air from Alaska and the Arctic over the ice growth regions in the coastal polynyas and vigorously drive the ice southward. In light ice years there are more storms, with storms propagating up the Siberian side. This exposes the ice to warm, moist air from the Pacific, drives the ice northward to the limits of the internal pack strength, and closes the polynya growth regions.

5. Relation of storm tracks to sea ice extent: quantitative results

Linear indices of storm patterns were developed by summing the number of storm centers within subregions of the Bering Sea. The first index is the number of storms for each ice growth season, October–February, in an eastern sector (Fig. 10) minus the number in the western sector. This index differentiates between southeast and northwest dominance of storm tracks. The second index is the number of storms for a given ice season that reach north of 59°N, which constitutes an index of the total number of storms penetrating the Bering Sea marginal ice zone. The third index is the amplitude of the first empirical orthogonal function (EOF) of storm track spatial correlation for October–February as shown in Fig. 11—this figure is qualitatively similar to the difference storm pattern for maximum-minus-minimum ice years shown in Fig. 9. The first EOF resolves 22.3% of the variance of the 23-year normalized storm track maps; only the first EOF pattern is statistically significant in terms of the Rule N test (Preisendorfer and Barnett, 1977; Overland and Preisendorfer, 1982). The fact that only the first EOF is significant may be a result of the small sample size, but also suggests that a northwest/southeast oscillation is the only major mode of storm track variability in the Bering Sea.

Results presented in Figs. 9 and 11 suggest that the number of storms penetrating the northern Bering Sea is correlated with western storm tracks. This is in fact the case; the correlation of index 1 with index 2 (negative implies western tracks) is $r = -0.43$ for the 22 years of record (Table 2). Ice year 1961/62 was excluded from the correlation because the ice extent is uncertain. The ice extent correlated with index 1 is $r = 0.71$, and the correlation with index 2 is $r = -0.30$. The correlations of both index 1 and the first EOF with the ice extent are significant at the 95% level. This suggests that ice extent is a func-

TABLE 2. Correlation of ice extent with three storm indices (ice year 1961/62 is not included).

	Ice extent (km)	E–W (Index 1)	North of 59°N (Index 2)	EOF (Index 3)
Mean	812.2	3.00	17.13	0.00
S.D.	114.5	39.82	5.60	0.958
Correlation with ice extent[1]		0.707	0.295	0.511

[1] A correlation of $r > 0.423$ is significant for the 5% critical point with 20 degrees of freedom.

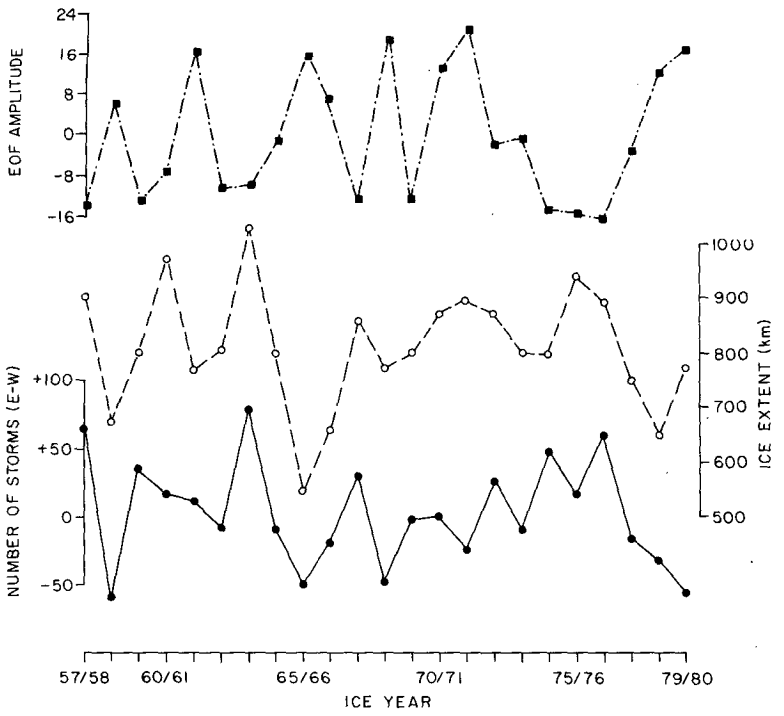

FIG. 12. Plot of the number of storms in the eastern sector minus the western sector (Index 1), the amplitude of the first EOF, and ice extent as a function of ice year.

tion primarily of storm track location. Fig. 12 plots index 1, the amplitude of the first EOF, and the maximum ice extent as a function of ice year.

The correlation between index 2 and the normalized ice extent is negative, as expected, but the correlation is low and not significant. The low correlation for index 2 is illustrated by the winter of 1963/64, the heaviest ice year in this record, which had an average number of storms over the northern and western sectors, but which showed an unusually large number of storms along the Alaska Peninsula.

6. Summary

Based on 23 years of data, we have constructed a storm track climatology for the Bering Sea in the winter season, October–March, in 2° latitude × 4° longitude grid cells. The seasonal trend is a decreased number of storms in January and February. There is a decrease in storms with latitude in all months. There is a tendency for two storm tracks, one parallel to the Aleutian Island chain and one curving northward along the Siberian coast. The ratio of the number of storms in the northern track relative to the southern track is greatest in January.

Maximum ice extents in the Bering Sea are computed for ice years 1957/58 to 1979/80. We estimate that the relative accuracy is better than ±50 km for ice years with satellite observations 1968/69 to 1979/80 and ±100 km before 1968/69, except for 1961/62, which had no direct observations published in the standard literature. The distribution of ice extents skews toward heavy ice years.

The difference in the storm-track patterns for the five heaviest and five lightest years shows a major difference in storm track. In light-ice years the cyclones propagate up the western side of the Bering Sea. Although no intensity information is associated with individual storms, the high correlation between east–west preference for storm track and ice extent suggests that there were a sufficient number of storms represented each winter for the influence of intensity variations of storms on ice extent to average out over any given winter.

Considering the possibility for errors in the various indices, we also conclude, on the basis of the high correlation between ice extent and storm track location, that meteorological steering of cyclones, determined primarily external to the Bering Sea (Walker and Bliss, 1932; Rogers, 1981), is the primary factor in determining interannual variability of sea ice extent. Further studies comparing patterns of upper level flow during heavy and light ice years and discussing the maintenance of significant anomalies in these patterns could establish a relationship between large-scale atmospheric features and regional ice extent.

Acknowledgments. This paper is a contribution to the Marine Services project at the Pacific Marine Environmental Laboratory. It was supported in part by the Bureau of Land Management through an interagency agreement with the National Oceanic and Atmospheric Administration, under which a multiyear program is being conducted to respond to the need for petroleum development on the Alaskan continental shelf, and is managed by the Outer Continental Shelf Environmental Assessment Program (OCSEAP). Much of the preliminary preparation of the storm track climatology was done by Sally A. Schoenberg.

REFERENCES

Barry, R. G., 1977: Study of climatic effects on fast ice extent and its seasonal decay along the Beaufort-Chukchi coasts. *Environmental Assessment of the Alaskan Continental Shelf*, Vol. 14, *Transport*, Environmental Research Laboratories, NOAA, Boulder, CO, 574–743. [NTIS PB-279110].

——, and A. H. Perry, 1973: *Synoptic Climatology, Methods and Application.* Methuen and Co., 553 pp.

Blackmon, M. L., J. M. Wallace, N. Lau and S. L. Mullen, 1977: An observational study of the Northern Hemisphere wintertime circulation. *J. Atmos. Sci.*, **34,** 1040–53.

Blasing, T. J., and H. C. Fritts, 1976: Reconstructing past climatic anomalies in North Pacific and western North America from tree-ring data. *Quat. Res.*, **6,** 563–579.

Brennecke, W. von, 1904: Beziehungen zwischen der Luftdruckverteilung und den Eisverhältnissen des Ostgrönländischen Meeres. *Ann. Hydrogr. Mar. Meteor.*, **32,** 49–62.

Crane, R. G., 1978: Seasonal variations of sea ice extent in the Davis Strait–Labrador Sea area and relationships with synoptic-scale atmospheric circulation. *Arctic*, **31,** 434–47.

Dunbar, M., 1967: The monthly and extreme limits of ice in the Bering Sea. *Physics of Snow and Ice*, Vol. 1, Inst. Low Temp. Sci., University of Hokkaido, Hokkaido, Japan, 687–703.

Hayden, B. P., 1981: Cyclone occurrence mapping: equal area or raw frequencies. *Mon. Wea. Rev.*, **109,** 168–172.

Johnson, C. M., 1980: Wintertime Arctic sea ice extremes and the simultaneous atmospheric circulation. *Mon. Wea. Rev.*, **108,** 1782–91.

Kinder, T. H., and J. D. Schumacher, 1981a: Hydrographic structure over the Continental Shelf of the southeastern Bering Sea. *The Eastern Bering Sea Shelf: Oceanography and Resources*, Vol. 1, D. W. Hood and J. A. Calder, Eds. [Government Printing Office (796-495), (Library of Congress 81-600035)], 31–52.

——, and ——, 1981b: Circulation over the Continental Shelf of the southeastern Bering Sea. *The Eastern Bering Sea Shelf: Oceanography and Resources*, Vol. 1, D. W. Hood and J. A. Calder, Eds. [Government Printing Office (796-495), (Library of Congress 81-600035)], 53–75.

Klein, W. H., 1957: Principal tracks and mean frequencies of cyclones and anticyclones in the northern hemisphere. Res. Pap. No. 40, U.S. Weather Bureau, 60 pp. [National Weather Service, Techniques Development Laboratory, Washington, DC 20233)].

McNutt, S. L., 1981: Ice conditions in the eastern Bering Sea from NOAA and LANDSAT imagery: Winter conditions 1974, 1976, 1977, 1979. NOAA Tech. Memo. ERL PMEL-24, 179 pp. [NTIS PB81-220188].

Muench, R. D., and K. Ahlnäs, 1976: Ice movement and distribution in the Bering Sea from March to June 1974. *J. Geophys. Res.*, **81,** 4467–76.

Niebauer, H. J., 1980: Sea ice and temperature variability in the eastern Bering Sea and the relation to atmospheric fluctuations. *J. Geophys. Res.*, **85,** 7507–15.

Overland, J. E., and T. R. Hiester, 1980: Development of a synoptic climatology for the northeast Gulf of Alaska. *J. Appl. Meteor.*, **19,** 1–14.

——, and R. W. Preisendorfer, 1982: A significance test for principal components applied to a cyclone climatology. *Mon. Wea. Rev.*, **110,** 1–4.

Pease, C. H., 1980: Eastern Bering Sea ice processes. *Mon. Wea. Rev.*, **108,** 2015–23.

——, and R. D. Muench, 1981: Cruise along ice edge in Bering Sea yields data on effects of gale. *Coastal Oceanography and Climatology News*, **3,** No. 4, 43–45.

Petterssen, S., 1956: *Weather Analysis and Forecasting*, Vol. 1. McGraw-Hill, 442 pp.

Preisendorfer, R. W., and T. P. Barnett, 1977: Significance tests for empirical orthogonal functions. *Preprints Fifth Conf. Probability and Statistics*, Las Vegas, Amer. Meteor. Soc., 169–172.

Putnins, P., 1966: The sequence of baric pressure patterns over Alaska. Studies on the Meteorology of Alaska. First Interim Report, Environmental Data Service, ESSA, Washington, DC, 57 pp. [NTIS AD-642679].

Rogers, J. C., 1978: Meteorological factors affecting interannual variability of summertime ice extent in the Beaufort Sea. *Mon. Wea. Rev.*, **106,** 890–97.

——, 1981: The North Pacific oscillation. *J. Climatology,* **1,** 39–57.

Schell, I. I., 1964: Interrelations of ice off northern Japan and the weather. *J. Meteor. Soc. Japan*, **42,** 174–85.

Schwerdtfeger, W., and S. Kachelhoffer, 1973: The frequency of cyclonic vortices over the southern ocean in relation to the extension of the pack ice belt. *Antarct. J. U.S.*, **8,** 234.

Suckling, P. W., and J. E. Hay, 1978: On the use of synoptic weather map typing to define solar radiation regimes. *Mon. Wea. Rev.*, **106,** 1521–1531.

Wadhams, P., 1981: The ice cover in the Greenland and Norwegian Sea. *Rev. Geophys. Space Phys.*, **19,** 345–93.

Walker, G. T., and E. W. Bliss, 1932: World Weather V. *Mem. Roy. Meteor. Soc.*, **4,** 53–84.

Walsh, J. E., and C. M. Johnson, 1979a: An analysis of Arctic sea ice fluctuations, 1953–77. *J. Phys. Oceanogr.*, **9,** 580–91.

——, and ——, 1979b: Interannual atmospheric variability and associated fluctuations in Arctic sea ice extent. *J. Geophys. Res.*, **84,** 6915–28.

Webster, B. D., 1981: A climatology of the ice extent in the Bering Sea. NOAA Tech. Memo. NWS AR 33, 38 pp. [National Weather Service, Alaska Region, Box 23, Anchorage].

White, W. B., and N. E. Clark, 1975: On the development of blocking ridge activity over the central north Pacific. *J. Atmos. Sci.*, **32,** 489–502.

Wiese, W., 1924: Polareis and atmosphärische schwankungen. *Geograf. Ann.*, **6,** 273–99.

Zishka, K. M., and P. J. Smith, 1980: The climatology of cyclones and anticyclones over north America and surrounding ocean environs for January and July, 1950–77. *Mon. Wea. Rev.*, **108,** 387–401.